

RESEARCH ARTICLE

Open Access



Differential diagnosis between hepatic alveolar echinococcosis and intrahepatic cholangiocarcinoma with conventional ultrasound and contrast-enhanced ultrasound

Zeng-Cheng Wa^{1†}, Ting Du^{1†}, Xian-Feng Li¹, Hui-Qing Xu¹, Qiu-Cuo Suo-Ang², Li-Da Chen³, Hang-Tong Hu³, Wei Wang³ and Ming-De Lu^{3,4*}

Abstract

Background: Misclassifications of hepatic alveolar echinococcosis (HAE) as intrahepatic cholangiocarcinoma (ICC) may lead to inappropriate treatment strategies. The aim of this study was to explore the differential diagnosis with conventional ultrasound and contrast-enhanced ultrasound (CEUS).

Methods: Sixty HAE lesions with 60 propensity score-matched ICC lesions were retrospectively collected. The 120 lesions were randomly divided into a training set ($n = 80$) and a testing set ($n = 40$). In the training set, the most useful independent conventional ultrasound and CEUS features was selected for differentiating between HAE and ICC. Then, a simplified US scoring system for diagnosing HAE was constructed based on selected features with weighted coefficients. The constructed US score for HAE was validated in both the training set and the testing set, and diagnostic performance was evaluated.

Results: Compared with ICC lesions, HAE lesions were mostly located in the right lobe and had mixed echogenicity, a pseudocystic appearance and foci calcifications on conventional ultrasound. On CEUS, HAE lesions showed more regular rim-like enhancement than ICC lesions and had late washout with a long enhancement duration. The simplified US score consisted of echogenicity, pseudocystic/calcification, bile duct dilatation, enhancement pattern, enhancement duration, and marked washout. In the testing set, the sensitivity, specificity, LR+, LR- and the area under the ROC curve for the score to differentiate HAE from ICC were 80.0, 81.3%, 4.27, 0.25 and 0.905, respectively.

(Continued on next page)

* Correspondence: lumd@live.com

[†]Zeng-Cheng Wa and Ting Du contributed equally to this work.

³Department of Medical Ultrasonics, Ultrasonics Artificial Intelligence X-Lab, Institute of Diagnostic and Interventional Ultrasound, The First Affiliated Hospital of Sun Yat-Sen University, 58 Zhongshan Road 2, Guangzhou 510080, People's Republic of China

⁴Department of Hepatobiliary Surgery, The First Affiliated Hospital of Sun Yat-Sen University, Guangzhou, China

Full list of author information is available at the end of the article



© The Author(s). 2020 **Open Access** This article is licensed under a Creative Commons Attribution 4.0 International License, which permits use, sharing, adaptation, distribution and reproduction in any medium or format, as long as you give appropriate credit to the original author(s) and the source, provide a link to the Creative Commons licence, and indicate if changes were made. The images or other third party material in this article are included in the article's Creative Commons licence, unless indicated otherwise in a credit line to the material. If material is not included in the article's Creative Commons licence and your intended use is not permitted by statutory regulation or exceeds the permitted use, you will need to obtain permission directly from the copyright holder. To view a copy of this licence, visit <http://creativecommons.org/licenses/by/4.0/>. The Creative Commons Public Domain Dedication waiver (<http://creativecommons.org/publicdomain/zero/1.0/>) applies to the data made available in this article, unless otherwise stated in a credit line to the data.

(Continued from previous page)

Conclusions: The US score based on typical features from both conventional ultrasound and CEUS could accurately differentiate HAE from ICC.

Keywords: Ultrasonography, Contrast-enhanced ultrasound, Echinococcosis, Cholangiocarcinoma, Diagnosis

Background

Alveolar echinococcosis (AE) is a globally distributed parasitic disease caused by an infection of *Echinococcus multilocularis* [1, 2]. The invasive growth pattern of AE resembles that of malignancy, and AE is acknowledged as one of the world's most lethal chronic parasitic conditions [3, 4]. Hepatic alveolar echinococcosis (HAE), AE at its most frequently involved site, constantly invades intrahepatic vessels, bile ducts and hilum with no clear histological margin between the parasitic tissue and the adjacent normal liver parenchyma [5]. HAE should be differentiated from other benign or malignant focal liver lesions, such as hemangioma, hepatapostema, and especially intrahepatic cholangiocarcinoma (ICC) [6]. As indicated by Stojkovic et al., the treatment decisions of 26/80 patients with HAE were based on an incorrect diagnosis [6]. Infiltrative HAE was commonly confused with ICC [6, 7]. These misclassifications of HAE as ICC may lead to the determination of inappropriate treatment strategies that are potentially harmful for patients.

Although the clinical significance of misclassifying HAE as ICC has been raised recently, the differential diagnosis has not been extensively studied. A study by Mueller et al. found that no or septal enhancement and matrix calcifications on Computed Tomography (CT) and Magnetic Resonance Imaging (MRI) offered the strongest discriminating potential between HAE and ICC with a high sensitivity and specificity [7]. Ultrasound (US) is accepted as the first-choice imaging modality in the diagnosis and follow-up for patients suspected to have HAE. Conventional ultrasound is extensively used, but contrast enhanced ultrasound (CEUS) has been implemented in clinical practice for the diagnosis of HAE [8–10] and can visualize the parenchymal microvasculature to provide more information for differential diagnoses. Since our first study on ICC in 2008, we have reported specific features of ICC for differentiate it from other liver lesions [11–13]. The aim of this study was to compare the imaging features of HAE and ICC both on conventional ultrasound and CEUS and to establish a diagnostic US score for HAE. To the best of our knowledge, no study has been focused on this topic.

Methods

Patients

Between January 2017 and March 2018, 57 patients with HAE with 60 lesions were retrospectively collected at

the ChengDuo County Hospital ($n = 43$) and QingHai Red Cross Hospital ($n = 14$), which are located in the major endemic region of Qinghai Province. The diagnosis for HAE was based on the criteria established by the World Health Organization Informal Working Group on Echinococcosis (WHO-IWGE) [3], and patients were included in this study if they had the following: 1) clinical and epidemiological history of living in pastoral areas with HAE, 2) conventional ultrasound and CEUS images, and 3) histologically or clinically proven HAE.

One hundred seventy patients with 170 ICC lesions were retrospectively collected at the First Affiliated Hospital of Sun Yat-sen University from January 2015 to March 2018. The inclusion criteria were patients with histologically proven ICC with integrated conventional ultrasound and CEUS images.

Propensity score matching was used to adjust for selection bias and to control for potential differences in the characteristics of patients. The variables for matching were sex and tumor size. HAE and ICC lesions were matched 1:1 using a three-digit matching algorithm with the nearest modality. Finally, 60 HAE lesions and 60 ICC lesions were analyzed in this study. There were 26 men and 34 women who were aged 38.9 ± 14.2 (mean \pm S.D.) years (range, 12–77 years) for HAE and 26 men and 34 women who were aged 58.5 ± 9.6 (mean \pm S.D.) years (range, 39–82 years) for ICC.

Conventional ultrasound and contrast-enhanced ultrasound

Ultrasound examinations were performed using Logiq S7 (GE Healthcare, Little Chalfont, UK) or ProSound F37 (Hitachi Medical Systems, Tokyo, Japan) at ChengDuo County Hospital or QingHai Red Cross Hospital. In the First Affiliated Hospital of Sun Yat-sen University, the Aplio 500 scanner (Toshiba Medical Systems, Tokyo, Japan) equipped with a 375BT convex transducer (frequency, 3.5 MHz) was used. Before the CEUS, a baseline grayscale ultrasound was performed to scan the entire liver. The imaging settings of the ultrasound scanner were optimized to obtain the best depiction of the target lesion. The diagnostic information including the diameter, echogenicity, shape, and margin of each lesion, was recorded. The contrast-specific imaging modes used in the present study were under a mechanical index of

0.07–0.12. After activating the contrast-specific imaging mode, 2.4 ml of SonoVue (Bracco, Milan, Italy) was administered intravenously in a bolus fashion and flushed with 5 ml 0.9% saline solution. The target lesion was observed continuously for 4–6 min, and the entire arterial and portal phases and several repetitions of the late phase were stored on the hard disk. The arterial, portal and late phases were defined as 0–40 s, 41–120 s and 121–360 s after the injection, respectively. All US examinations were performed by two experienced radiologists (W.Z.C. and D.T., each with more than 4 years of experience in liver CEUS). The digital cine clips of the conventional ultrasound and the entire CEUS examination were stored on a hard disk incorporated in the scanner, and the image files were transferred to a removable disk for subsequent analysis. The data disk was sent to the ultrasound department of the First Affiliated Hospital of Sun Yat-Sen University for further data exploration.

Image analysis

Two experienced radiologists (C.L.D. and W.W. with at least 8 years of experience in liver CEUS) randomly reviewed all the cine loops offline on screen in consensus. Both readers were not involved in the original examinations and were asked to document the following characteristic signs of lesion on conventional ultrasound: location, size, echogenicity, pseudocystic appearance, calcification of the lesion, and bile duct dilatation (diameter of intra-hepatic bile duct > 3 mm, or extra-hepatic bile duct > 8 mm).

The characteristic signs on CEUS were evaluated as follows [13–15]: a) enhancement level -- hyper-, iso- or hypoenhancing relative to the adjacent normal liver parenchyma; b) no enhancement -- no appearance of microbubble signals in the lesion; c) heterogeneous enhancement -- lesion enhancement with a different level of echogenicity; d) regular rim enhancement -- microbubble signals detected at a regular peripheral portion of the lesion; e) irregular rim enhancement -- microbubble signals detected at an irregular peripheral portion of the lesion; f) enhancement start time, washout time, and enhancement duration; g) lesion shape and margin; and h) washout level -- mild, moderate, or marked washout relative to the adjacent liver parenchyma.

Statistical analysis

Statistical analysis and the random sequence numbers were performed by using SPSS 16.0 software (SPSS Inc., Chicago, IL, USA) and R software (R Foundation for Statistical Computing, version 3.2.5, <http://www.rproject.org/>, Austria). Data are presented as the mean ± standard deviation (SD) and percentage (%). *P* < 0.05 was considered to indicate statistical significance. The association between lesion size and imaging features was

Table 1 Characteristics on US between HAE and ICC

Imaging Features on US	Total(n = 120)		P*
	HAE (n = 60)	ICC (n = 60)	
Conventional US			
Location			0.002
Right lobe	50 (83.3)	33 (55.0)	
Left lobe	10 (16.7)	27 (45.0)	
Lesion size			0.851
≤ 5.0 cm	22 (36.7)	24 (40.0)	
> 5.0 cm	38 (63.3)	36 (60.0)	
Echogenicity			0.000
Hyper or Iso	10 (16.7)	7 (11.6)	
Mixed	43 (71.7)	19 (31.7)	
Hypo	7 (11.6)	34 (56.7)	
Margin			1.000
Clear	28 (46.7)	28 (46.7)	
Unclear	32 (53.3)	32 (53.3)	
Bile duct dilatation	2 (3.3)	21 (35.0)	0.000
Pseudocystic appearance	14 (23.3)	1 (1.7)	0.000
Calcification	29 (48.3)	0 (0)	0.000
CEUS			
Arterial phase			0.008
Hyper-	39 (65.0)	50 (83.3)	
Iso-	10 (16.7)	9 (15.0)	
Hypo- or Non-	11 (18.3)	1 (1.7)	
Enhancement pattern			0.000
Regular rim	53 (88.3)	6 (10.0)	
Irregular rim	6 (10.0)	29 (48.4)	
Heterogeneous	1 (1.7)	14 (23.3)	
Homogeneous	0 (0)	11 (18.3)	
Portal phase			0.000
Hyper-	1 (1.7)	0 (0)	
Iso-	19 (31.6)	1 (1.7)	
Hypo- or Non-	40 (66.7)	59 (98.3)	
Late phase			0.000
Hyper-	1 (1.7)	0 (0)	
Iso-	16 (26.6)	1 (1.7)	
Hypo- or Non-	43 (71.7)	59 (98.3)	
Enhancement duration#	201.7 ± 146.4	33.5 ± 59.5	0.000
Marked wash-out	15 (25.0)	44 (73.3)	0.000

Note.---Unless otherwise indicated, data are number of nodules, with percentages in parentheses

*Statistical analysis using χ^2 or Fisher's exact test demonstrate differences between HAE and ICC

Data are means ± standard deviations

HAE Hepatic alveolar echinococcosis; ICC Intrahepatic cholangiocarcinoma; US Ultrasound; CEUS Contrast enhanced ultrasound

assessed using χ^2 or Fisher's exact tests. Student's t-test was used to compare lesion size within the same characteristic imaging findings.

The 120 lesions were randomly divided into a training set ($n = 80$) and a testing set ($n = 40$). In the training set, the method of least absolute shrinkage and selection

Table 2 Characteristics on US in the training and testing set

Imaging Features on US	Training set (n = 80)		Testing set (n = 40)		P*
	HAE(n = 36)	ICC(n = 44)	HAE(n = 24)	ICC(n = 16)	
Conventional US					
Location					
Right lobe	30 (83.3)	24 (54.5)	20 (83.3)	9 (56.3)	0.252
Left lobe	6 (16.7)	20 (45.5)	4 (16.7)	7 (43.7)	0.393
Lesion size					
≤ 5.0 cm	14 (38.9)	17 (38.6)	8 (33.3)	7 (43.7)	0.755
> 5.0 cm	22 (61.1)	27 (61.4)	16 (66.7)	9 (56.3)	0.145
Echogenicity					
Hyper or Iso	5 (13.8)	3 (6.8)	5 (20.8)	4 (25.0)	1.000
Mixed	25 (69.4)	14 (31.8)	18 (75.0)	5 (31.3)	0.271
Hypo	6 (16.7)	27 (61.4)	1 (4.2)	7 (43.7)	1.000
Margin					
Clear	17 (47.2)	20 (45.5)	11 (45.8)	8 (50.0)	0.573
Unclear	19 (52.8)	24 (54.5)	13 (54.2)	8 (50.0)	0.287
Bile duct dilatation	1 (2.8)	16 (36.4)	1 (4.2)	5 (31.3)	0.462
Pseudocystic appearance	9 (25.0)	1 (2.3)	5 (20.8)	0 (0)	1.000
Calcification	16 (44.4)	0 (0)	13 (54.2)	0 (0)	NA
CEUS					
Arterial phase					
Hyper-	23 (63.9)	35 (79.5)	16 (66.7)	15 (93.8)	0.370
Iso-	5 (13.9)	8 (18.2)	5 (20.8)	1 (6.3)	0.141
Hypo- or Non-	8 (22.2)	1 (2.3)	3 (12.5)	0 (0)	1.000
Enhancement pattern					
Regular rim	33 (91.7)	4 (9.0)	20 (8.3)	2 (12.5)	1.000
Irregular rim	2 (5.6)	22 (50.0)	4 (16.7)	7 (43.8)	0.063
Heterogeneous	1 (2.7)	9 (20.5)	0 (0)	5 (31.2)	1.000
Homogeneous	0 (0)	9 (20.5)	0 (0)	2 (12.5)	NA
Portal phase					
Hyper-	1 (2.8)	0 (0)	0 (0)	0 (0)	NA
Iso-	9 (25.0)	0 (0)	10 (41.7)	1 (6.3)	1.000
Hypo- or Non-	26 (72.2)	44 (100)	14 (58.3)	15 (93.7)	0.3670
Late phase					
Hyper-	1 (2.8)	0 (0)	0 (0)	0 (0)	NA
Iso-	7 (19.4)	0 (0)	9 (37.5)	1 (6.3)	1.000
Hypo- or Non-	28 (77.8)	44 (100)	15 (62.5)	15 (93.7)	0.380
Enhancement duration#	197.4 ± 138.2	23.7 ± 16.2	205.9 ± 137.6	19.9 ± 5.3	
Marked wash-out	10 (27.8)	32 (72.7)	5 (20.8)	12 (75.0)	0.745

Note:---Unless otherwise indicated, data are number of nodules, with percentages in parentheses

Data are means± standard deviations

*Statistical analysis using χ^2 or Fisher's exact test demonstrate differences between the training set and testing set. NA Not available

HAE Hepatic alveolar echinococcosis; ICC Intrahepatic cholangiocarcinoma; US Ultrasound; CEUS Contrast enhanced ultrasound

operator (LASSO) regularized regression was used to select the most useful independent conventional ultrasound and CEUS features for differentiating between HAE and ICC, respectively. Then, a US scoring system for diagnosing HAE that including features from both conventional ultrasound and CEUS was constructed for each patient using a linear equation of the combined selected features that were weighted by their respective coefficients. The constructed US scoring system for HAE was validated in both the training set and the testing set. The receiver operating characteristic (ROC) curve for differentiating between HAE and ICC was analyzed by calculating the area under the curve (AUC). The ROC curve was plotted to demonstrate the diagnostic performance of CEUS in the testing set. Sensitivity, specificity, positive predictive value (PPV), and negative predictive value (NPV) were calculated with an optimal cutoff value that maximized the sum of sensitivity and specificity.

Results

Conventional ultrasound features for HAE and ICC

All HAE and ICC lesions were confirmed by pathologic evaluation after surgery. Ten (16.7%) of the 60 observed

HAE lesions were located in the left lobes of the livers, and 50 (83.3%) were in the right lobes. There were 27 (27/60, 45.0%) and 33 (33/60, 55.0%) ICC lesions located in the left and right lobes, respectively ($P = 0.002$). Forty-three (71.7%) HAE lesions showed mixed echogenicity, and only 7 HAE lesions showed hypoechogenicity; 34 (56.7%) ICC lesions showed hypoechogenicity. Only 2 (3.3%) HAE lesions were accompanied by bile duct dilatation in the liver, but 21 (35.0%) ICC lesions were accompanied by bile duct dilatation ($P = 0.000$). A pseudocystic appearance was observed for 14 (23.3%) HAE lesions but only for 1 (1.7%) ICC lesion. Notably, foci calcifications were observed in 29 (48.3%) HAE lesions but not in any ICC lesions ($P = 0.000$). Details of the HAE lesions and ICC lesions in the control group are listed in Table 1. Statistical analyses demonstrated that there were no significant differences between the training set and testing set for all US features (Table 2).

CEUS features for HAE and ICC

The enhancement patterns of 60 HAE lesions after an injection of SonoVue contrast agent are summarized in Table 1-2. The number of HAE lesions that showed hyper-, iso-, and hypoenhancement in the

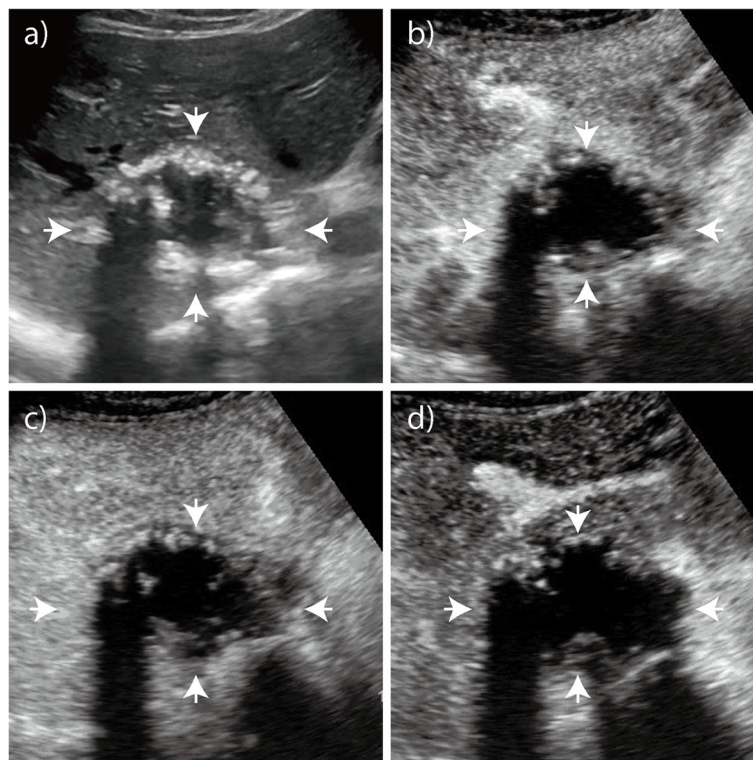


Fig. 1 Hepatic alveolar echinococcosis (HAE). **a** Baseline ultrasound image shows a nodule with mixed echogenicity in the right lobe of the liver that is 5.8 cm in diameter. **b** On CEUS, arterial phase image obtained 19 s after administering the contrast agent shows a rim-like hyperenhancement of the lesion. **c - d** Portal and late phase images obtained 96 s and 129 s after administering the contrast agent, respectively. The nodule is hypoechoic with respect to the surrounding liver

arterial phase were 39 (65.0%), 10 (16.7%), and 11 (18.3%), respectively; the number of ICC lesions that showed hyper-, iso-, and hypoenhancement were 50 (83.3%), 9 (15.0%), and 1 (1.7%), respectively ($P = 0.008$). Most HAE lesions exhibited regular peritumoral enhancement ($n = 53$, 88.3%). The areas of enhancement were primarily seen at the peripheral portions of the lesions and appeared as regular rim-like enhancement. The inner edge of the enhanced area was lumpy and strip-like and hardly extended to the central portion of the nodules (Figs. 1, 2, 3). However, irregular rims ($n = 29$, 48.3%) and heterogeneous or homogeneous enhancement ($n = 25$, 41.7%) were more commonly observed in ICC lesions than in HAE lesions ($P = 0.000$). In the portal and late phase, the enhanced areas in the HAE nodules faded out slowly (long enhancement duration: 201.7 s), but all ICC nodules faded out rapidly (short enhancement duration: 33.5 s). Forty lesions appeared with hypoenhancement, and 16 were iso-enhanced in the late phase. While more ($n = 59$, 98.3%) ICC lesions appeared hypo-enhanced in the late phase than HAE lesions, more ($n = 44$, 73.3%) ICC lesions showed marked washout than HAE lesions ($P = 0.000$) (Fig. 4).

US score for diagnosing HAE

In the training set, LASSO regression analysis demonstrated that the selected conventional ultrasound and CEUS variables for differentiation were echogenicity, pseudocystic/calcification, bile duct dilatation, enhancement pattern, enhancement duration, and marked wash-out. In order to ensure reproducibility and easy access to clinical practice, a simplified scoring system is proposed, which gives assigned scores based on the coefficient of selected features (Table 3). For example, if an HAE lesion showed mixed echogenicity (1 points) with a pseudocystic appearance and calcifications (2 points) without bile duct dilatation (-1 points) on conventional ultrasound, but the CEUS showed regular rim enhancement (1 point) with an enhancement duration of 150 s (1 point) and no marked washout (-1 point), then the US total score would be 3. The mean US scores for HAE and ICC patients were 2.48 and 0.40, respectively, and the ROC analysis showed that the optimal cut-off value for differentiation was 1.0. If the US score for a patient was higher than this cut-off value, the diagnosis would be HAE; conversely, if the US score was lower than this cut-off value, the diagnosis would be ICC. Since the US

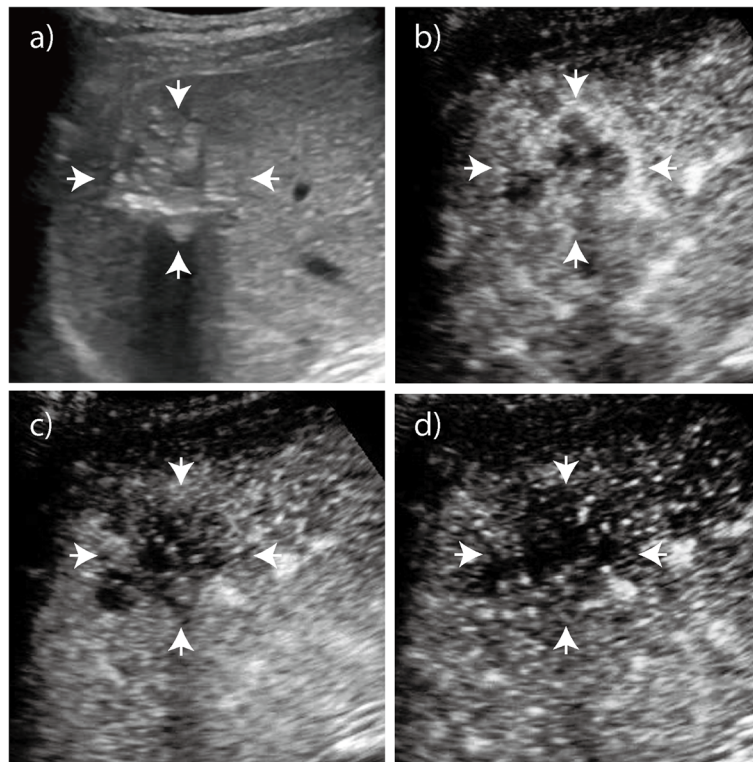


Fig. 2 Hepatic alveolar echinococcosis (HAE). **a** Baseline ultrasound image shows a nodule with mixed echogenicity in the right lobe of the liver that is 5.0 cm in diameter. **b** On CEUS, arterial phase image obtained 15 s after administering the contrast agent shows diffuse heterogeneous hyperenhancement of the lesion. **c - d** Portal and late phase images obtained at 43 s and 131 s after administering the contrast agent, respectively. The nodule is hypochoic with respect to the surrounding liver

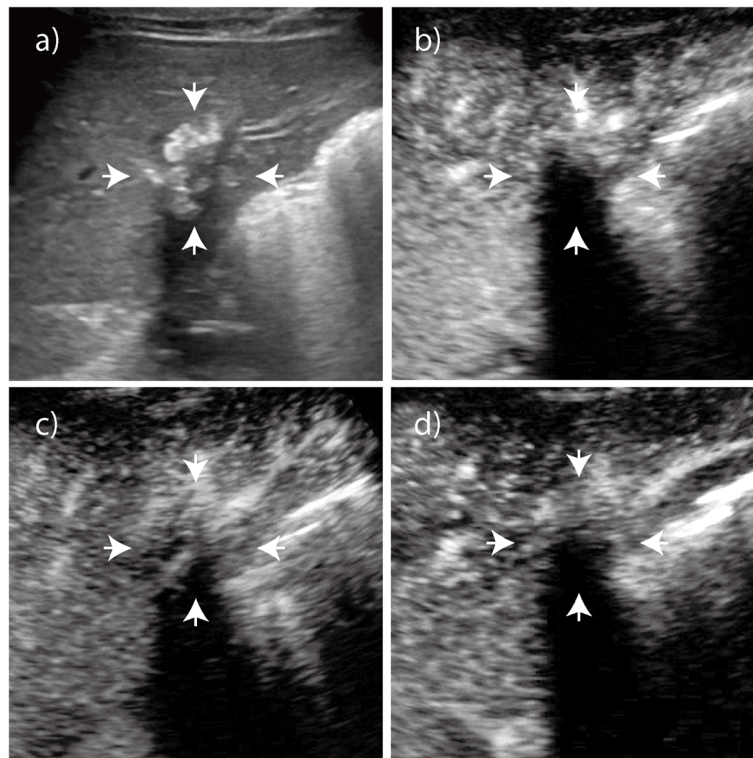


Fig. 3 Hepatic alveolar echinococcosis (HAE). **a** Baseline ultrasound image shows a nodule with hyperechogenicity with macrocalcifications in the right lobe of the liver that is 2.9 cm in diameter. **b - d** On CEUS, no microbubble signals appear in the lesion in any of the three phases

score for this patient (3.0) was higher than the cut-off value of 1.0, the diagnosis was HAE.

Diagnostic performance of the US score

In the training set, the diagnostic performance of the US score demonstrated that the sensitivity, specificity, LR+, LR- and AUC were 82.5, 86.4%, 6.05, 0.20 and 0.913, respectively. In the testing set, the sensitivity, specificity, LR+, LR- and AUC were 80.0, 81.3%, and 0.905, respectively. In the subgroup of lesions ≤5.0 cm, the sensitivity, specificity, LR+, LR- and AUC were 72.7, 91.7%, and 0.917, respectively. In the three cohorts, the diagnostic performances were excellent (all AUCs > 0.90, Table 4). The diagnostic performance of simple combined BUS and CEUS score was better than that of BUS or CEUS score alone (Table 4).

Discussion

In our study, the typical conventional ultrasound and CEUS features of HAE such as hyper or mixed echogenicity with a pseudocystic appearance or calcifications on conventional ultrasound as well as regular rim enhancement and long enhancement duration on CEUS were combined; based on these features, we first developed a diagnostic US score for HAE that had an excellent accuracy of 95.0% and a perfect sensitivity of 100.0% in the testing cohort.

Conventional ultrasound could provide informative features for differentiating between HAE and ICC. In our study, most (88.3%) HAE lesions showed hyper or mixed echogenicity. A pseudocystic appearance or diffuse foci calcifications were observed in about 70% of the HAE lesions. However, ICC lesions commonly showed hypoechogenicity without cystic or necrotic areas [16]. Calcifications with/without acoustic shadowing were sometimes shown inside ICC lesions, but the foci calcifications were usually clustered with solid hypoechogenicity. Moreover, intrahepatic biliary dilatation was more commonly present in ICC than in HAE.

In recent years, CEUS has been introduced as a promising imaging technique for the diagnosis of HAE [9, 10, 17]. With the progress in contrast agents and contrast-specific imaging techniques, the parenchymal microvasculature of HAE lesions can be dynamically visualized on CEUS. Ehrhardt et al. compared the imaging features of HAE lesions on CEUS with those of fluorodeoxyglucose positron emission tomography (FDG-PET) [18]. The authors concluded that CEUS could assess the activity of HAE, and the findings with CEUS were consistent with the results of FDG-PET. In our study, 95.4% of the lesions were detected with enhancement, which correlates with active texture or an inflammatory reaction belt surrounding the lesion [10].

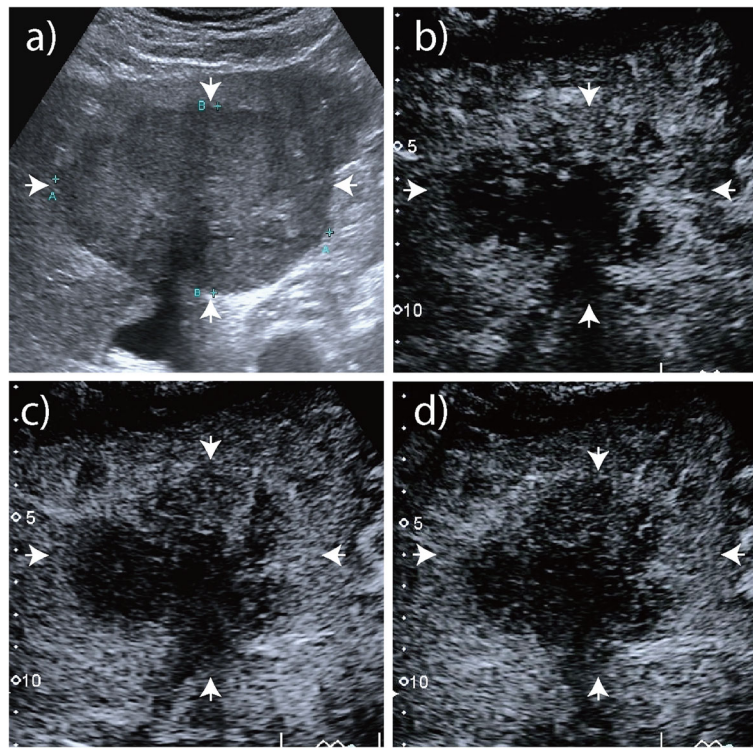


Fig. 4 Intrahepatic cholangiocarcinoma (ICC). **a** Baseline ultrasound image shows a nodule with hypoechogenicity without macrocalcifications in the right lobe of the liver that is 8.7 cm in diameter. **b** In arterial phase on CEUS, the tumor appeared as irregular rim enhancement. **c - d** In portal and late phase, it faded out rapidly and showed marked washout

Most HAE lesions had regular rim enhancement and no enhancement in the center of lesion mass in the arterial and portal venous phases [17]. In our study, 84.8% of the lesions had this individual sign, which is similar to the percentage in previous reports (64–100%) [9, 17]. However, the rim enhancement pattern was also reported to be commonly detected in ICC lesions at a high rate of 68.5% [12]. In this study, we found that the rim enhancement of HAE lesions was regular and thin, which may be due to the enhancement of the alveolar wall. In contrast, the rim enhancement of ICC lesions was irregular and thicker than the linear rim of HAE lesions, which may be due to the infiltrative and abundant tumor cells at the periphery of the tumor.

In addition to the above typical CEUS feature, no enhancement, due to the vesicle structures, or diffuse heterogeneous hyperenhancement were also reported to be parts of the enhancement patterns for HAE lesions [9, 10]. These results are consistent with those of Cai et al’s study on evaluating 17 HAE lesions with CEUS [8]. Additionally, late or no obvious washout of the alveolar wall were suggestive features of HAE. However, diffuse heterogeneous enhancement was more common in ICC than in HAE. Other differences between ICC and HAE included the following: the enhancement of ICC lesions faded out more rapidly than that of HAE lesions, and most ICC lesions showed marked washout in the late phase.

The diagnostic performance of our US score for differentiating between these two entities demonstrated that

Table 3 The Formation of an Equation for the US Score

Selected features	Coefficient	Signs	Assigned Score
Echogenicity	-0.11112163	Mixed-echogenicity	-1
Pseudocystic/calcification	1.12745008	Pseudocystic/calcification	1
Bile duct dilatation	-0.32246004	Bile duct dilatation	-1
Enhancement pattern	0.40994879	Regular rim	1
Enhancement duration	0.00372324	> 60s	1
Marked washout	-0.52185663	Marked washout	-1

Table 4 Diagnostic Performance of BUS and/or CEUS for Differentiating between HAE and ICC

	Sensitivity ^a	95% CI ^a	Specificity ^a	95% CI ^a	AUC	95% CI	LR+	LR-
BUS + CEUS score								
Training set	82.5	67.2–92.7	86.4	72.6–94.8	0.913	0.832–0.964	6.05	0.20
Testing set	80.0	56.3–94.3	81.3	54.4–96.0	0.905	0.760–0.977	4.27	0.25
≤ 5.0 cm	72.7	49.8–89.3	91.7	73.0–99.0	0.912	0.791–0.975	8.73	0.30
BUS score								
Training set	67.5	50.9–81.4	100.0	92.0–100.0	0.886	0.798–0.945	NA	0.33
Testing set	60.0	36.1–80.9	100.0	79.4–100.0	0.925	0.786–0.986	NA	0.40
≤ 5.0 cm	45.5	24.4–67.8	100.0	85.8–100.0	0.875	0.744–0.954	NA	0.55
CEUS score								
Training set	82.5	67.2–92.7	65.9	50.1–79.5	0.777	0.673–0.861	2.42	0.27
Testing set	65.0	40.8–84.6	68.9	41.3–89.0	0.717	0.543–0.854	2.08	0.51
≤ 5.0 cm	72.7	49.8–89.3	75.0	53.3–90.2	0.773	0.625–0.883	2.91	0.36

^a Numbers are percentages

HAE Hepatic alveolar echinococcosis; ICC Intrahepatic cholangiocarcinoma; CEUS Contrast enhanced ultrasound; AUC Area under the curve; PPV Positive predictive value; NPV Negative predictive value

its specificity was high (86.4%), and the AUC was excellent (0.9qe). The subgroup analysis for lesions smaller than 5.0 cm indicated that the differentiation performance of the US score was also high, with a sensitivity, specificity, and AUC of 72.7, 91.7%, and 0.912, respectively.

Our study had some limitations. First, the sample size of our study was relatively small, and ossification and hemangioma-like patterns in the HAE cases were rare. Consequently, the differentiation performance of the diagnostic score might be limited. Second, our study was retrospective, and further prospective studies are necessary, especially to explore if prognosis correlates with the different enhancement patterns of HAE. Future research about comparing the diagnostic performance of CEUS and CT/MRI will be also needed. Finally, CEUS may suffer from some of the same limitations as conventional sonography. For example, it may be difficult to detect lesions near the diaphragm dome or with a fatty liver background. Furthermore, the arterial phase lasts less than 1 min, so only one lesion or several lesions on the same plane can be observed with a single injection of contrast agent.

Conclusion

The US score based on typical features from both conventional ultrasound and CEUS could accurately differentiate HAE from ICC. The enhancement pattern of HAE lesions on CEUS could provide informative advice for treatment decisions and be introduced as the standard modality for diagnosing HAE in patients who live in pastoral areas.

Abbreviations

AE: Alveolar echinococcosis; HAE: Hepatic alveolar echinococcosis; ICC: Intrahepatic cholangiocarcinoma; US: Ultrasound; CEUS: Contrast enhanced ultrasound; WHO-IWGE: World health organization informal working group on echinococcosis; SD: Standard deviation; LASSO: Least absolute shrinkage and selection operator; ROC: Receiver operating characteristic; AUC: Area under the curve; PPV: Positive predictive value; NPV: Negative predictive value; FDG-PET: Fluorodeoxyglucose positron emission tomography; CT: Computed tomography; MRI: Magnetic resonance imaging

Acknowledgements

Not applicable.

Authors' contributions

Conception and design: M.D.L., W.W. Development of methodology: Z.C.W., T.D., M.D.L., W.W. Acquisition of data (e.g., collected patients, performed imaging): Z.C.W., T.D., X.F.L., H.Q.X., Q.C.S.A. Analysis and interpretation of data (e.g., computational analysis, statistical analysis): L.D.C., H.T.H., W.W. Editing and review of the manuscript: all authors. Study supervision: M.D.L., W.W. All authors have read and approved the manuscript.

Funding

This work was supported by the National Nature Science Foundation of China (No: 81471672 and 81601500), Guangdong Natural Science Foundation (No: 2017A030313661), and the Guangdong Science and Technology Foundation (No: 2017A020215195). The funding bodies played no role in the design of the study and collection, analysis, and interpretation of data and in writing the manuscript.

Availability of data and materials

The datasets generated and analyzed in this study are available upon reasonable request by the corresponding author. Email: lumd@live.com

Ethics approval and consent to participate

This study was approved by the institutional review board at the corresponding author's institution (the First Affiliated Hospital of Sun Yat-Sen University), and informed consent was obtained from all patients. The consent obtained from study participants was verbal because this retrospective study has been approved by the ethics committee at the corresponding author's institution.

Consent for publication

Not applicable.

Competing interests

The authors declare that they have no competing interests.

Author details

¹Department of Medical Ultrasonics, Qinghai Red Cross Hospital, Xining, China. ²Department of Medical Ultrasonics, People's Hospital of Chengduo County, Yushu Prefecture, China. ³Department of Medical Ultrasonics, Ultrasonics Artificial Intelligence X-Lab, Institute of Diagnostic and Interventional Ultrasound, The First Affiliated Hospital of Sun Yat-Sen University, 58 Zhongshan Road 2, Guangzhou 510080, People's Republic of China. ⁴Department of Hepatobiliary Surgery, The First Affiliated Hospital of Sun Yat-Sen University, Guangzhou, China.

Received: 12 September 2019 Accepted: 19 August 2020

Published online: 27 August 2020

References

- Kern P, Wen H, Sato N, Vuitton DA, Gruener B, Shao Y, Delabrousse E, Kratzer W, Bresson-Hadni S. WHO classification of alveolar echinococcosis: principles and application. *Parasitol Int.* 2006;55(Suppl):S283–7.
- Casulli A, Who-Iwge SGO: Meeting of the WHO informal working group on Echinococcosis (WHO-IWGE). 2017.
- Brunetti E, Kern P, Vuitton DA. Writing panel for the W-I: expert consensus for the diagnosis and treatment of cystic and alveolar echinococcosis in humans. *Acta Trop.* 2010;114(1):1–16.
- McManus DP, Gray DJ, Zhang W, Yang Y. Diagnosis, treatment, and management of echinococcosis. *BMJ.* 2012;344:e3866.
- Liu W, Delabrousse E, Blagosklonov O, Wang J, Zeng H, Jiang Y, Wang J, Qin Y, Vuitton DA, Wen H. Innovation in hepatic alveolar echinococcosis imaging: best use of old tools, and necessary evaluation of new ones. *Parasite.* 2014;21:74.
- Stojkovic M, Mickan C, Weber TF, Junghans T. Pitfalls in diagnosis and treatment of alveolar echinococcosis: a sentinel case series. *BMJ Open Gastroenterol.* 2015;2(1):e000036.
- Mueller J, Stojkovic M, Berger AK, Rosenberger KD, Schlett CL, Kauczor HU, Junghans T, Weber TF. How to not miss alveolar echinococcosis in hepatic lesions suspicious for cholangiocellular carcinoma. *Abdom Radiol (NY).* 2016; 41(2):221–30.
- Cai DM, Wang HY, Wang XL, Jiang Y, Luo Y, Li YZ. Ultrasonographic findings of small lesion of hepatic alveolar echinococcosis. *Acta Trop.* 2017;174:165–70.
- Zhang H, Liu ZH, Zhu H, Han Y, Liu J, Deng LQ. Analysis of contrast-enhanced ultrasound (CEUS) and pathological images of hepatic alveolar echinococcosis (HAE) lesions. *Eur Rev Med Pharmacol Sci.* 2016; 20(10):1954–60.
- Zeng H, Wang J, Xie W, Liu W, Wen H. Assessment of early hepatic echinococcus multilocularis infection in rats with real-time contrast-enhanced ultrasonography. *Ultrasound Med Biol.* 2012;38(11):1982–8.
- Chen LD, Xu HX, Xie XY, Lu MD, Xu ZF, Liu GJ, Liang JY, Lin MX. Enhancement patterns of intrahepatic cholangiocarcinoma: comparison between contrast-enhanced ultrasound and contrast-enhanced CT. *Br J Radiol.* 2008;81(971):881–9.
- Liu GJ, Wang W, Lu MD, Xie XY, Xu HX, Xu ZF, Chen LD, Wang Z, Liang JY, Huang Y, et al. Contrast-enhanced ultrasound for the characterization of hepatocellular carcinoma and intrahepatic Cholangiocarcinoma. *Liver Cancer.* 2015;4:241–52.
- Chen LD, Ruan SM, Lin Y, Liang JY, Shen SL, Hu HT, Huang Y, Li W, Wang Z, Xie XY, et al. Comparison between M-score and LR-M in the reporting system of contrast-enhanced ultrasound LI-RADS. *Eur Radiol.* 2019;29(8): 4249–57.
- Liu GJ, Lu MD, Xie XY, Xu HX, Xu ZF, Zheng YL, Liang JY, Wang W. Real-time contrast-enhanced ultrasound imaging of infected focal liver lesions. *J Ultrasound Med.* 2008;27(4):657–66.
- Wang W, Chen LD, Lu MD, Liu GJ, Shen SL, Xu ZF, Xie XY, Wang Y, Zhou LY. Contrast-enhanced ultrasound features of histologically proven focal nodular hyperplasia: diagnostic performance compared with contrast-enhanced CT. *Eur Radiol.* 2013;23(9):2546–54.
- Chen LD, Xu HX, Xie XY, Xie XH, Xu ZF, Liu GJ, Wang Z, Lin MX, Lu MD. Intrahepatic cholangiocarcinoma and hepatocellular carcinoma: differential diagnosis with contrast-enhanced ultrasound. *Eur Radiol.* 2010;20(3):743–53.
- Tao S, Qin Z, Hao W, Yongquan L, Lanhui Y, Lei Y. Usefulness of gray-scale contrast-enhanced ultrasonography (SonoVue(R)) in diagnosing hepatic alveolar echinococcosis. *Ultrasound Med Biol.* 2011;37(7):1024–8.
- Ehrhardt AR, Reuter S, Buck AK, Haenle MM, Mason RA, Gabelmann A, Kern P, Kratzer W. Assessment of disease activity in alveolar echinococcosis: a comparison of contrast enhanced ultrasound, three-phase helical CT and [(18) F] fluorodeoxyglucose positron emission tomography. *Abdom Imaging.* 2007;32(6):730–6.

Publisher's Note

Springer Nature remains neutral with regard to jurisdictional claims in published maps and institutional affiliations.

Ready to submit your research? Choose BMC and benefit from:

- fast, convenient online submission
- thorough peer review by experienced researchers in your field
- rapid publication on acceptance
- support for research data, including large and complex data types
- gold Open Access which fosters wider collaboration and increased citations
- maximum visibility for your research: over 100M website views per year

At BMC, research is always in progress.

Learn more [biomedcentral.com/submissions](https://www.biomedcentral.com/submissions)

